

# Modeling of Electron Mobility in Strained Si Devices

S. Dhar, H. Kosina, V. Palankovski, E. Ungersböck, and S. Selberherr

Institut für Mikroelektronik, Technische Universität Wien, Gusshausstrasse 27-29, A-1040 Vienna, Austria

Phone: +43-1-58801-36018, Fax: +43-1-58801-36099, E-Mail: [dhar@iue.tuwien.ac.at](mailto:dhar@iue.tuwien.ac.at)

**Abstract**— A model describing the anisotropic electron mobility in strained Si has been developed. Our analytical model includes the effect of strain-induced splitting of the conduction band valleys in Si, inter-valley scattering, and doping dependence. Monte Carlo simulations were performed to verify the results for the complete range of Ge contents and for a general orientation of the SiGe buffer. Our mobility model is suitable for implementation into a conventional TCAD simulation tool.

**Keywords**—strained Si, SiGe, mobility model, inter-valley scattering, Technology CAD, Monte Carlo simulations

## I. INTRODUCTION

Strained Si material has emerged as a strong contender for developing transistors for the next generation electronics. Strain lifts the degeneracy of the valence and conduction bands which can be used to deliver superior transport properties in comparison to bulk Si. Transistors fabricated using strained Si layers have reported larger drive currents capabilities [1] [2] due to the enhanced electron and hole mobilities. Possible applications of strained Si include high-speed products like microprocessors and low-power circuits in wireless communications.

To enable predictive simulations using TCAD tools a reliable set of models for the Si/SiGe material system is required. This work suggests a model to describe the perpendicular mobility and the anisotropy of the in-plane mobility of electrons in strained Si. The model includes valley splitting for a given strain tensor, the effect of inter-valley scattering, and the doping dependence. Monte Carlo simulations accounting for the splitting of anisotropic conduction band valleys were performed to verify the analytical model for the complete range of germanium contents and for a general orientation of the SiGe substrate.

## II. PHYSICAL BACKGROUND

Strained Si layers are achieved by growth on SiGe buffers. Due to the lattice mismatch, a pseudomorphically grown Si layer on a relaxed SiGe buffer experiences a biaxial tensile strain, provided that the layer thickness is below a critical value to prevent strain relaxation. Recently other methods for generating strain in Si have been proposed [3] [4]. Biaxial strain leads to a modification of the conduction band, as shown in Fig. 1. The 6-fold degenerate  $\Delta_6$ -valleys in Si is being split into 2-fold degenerate  $\Delta_2$  valleys (lower in energy) and 4-fold degenerate  $\Delta_4$  valleys (higher in energy). The lower in-plane effective mass of electrons in the  $\Delta_2$  valleys and the reduction of inter-valley phonon scattering lead to an enhancement of electron mobility.

erate  $\Delta_6$ -valleys in Si is being split into 2-fold degenerate  $\Delta_2$  valleys (lower in energy) and 4-fold degenerate  $\Delta_4$  valleys (higher in energy). The lower in-plane effective mass of electrons in the  $\Delta_2$  valleys and the reduction of inter-valley phonon scattering lead to an enhancement of electron mobility.

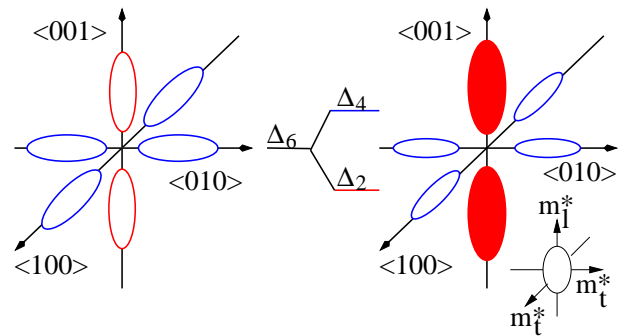


Fig. 1. Conduction band splitting in tensile-strained Si (right) compared to unstrained Si (left).

## III. THEORETICAL DERIVATION

To model the electron mobility in strained Si, including the effect decreasing inter-valley scattering rate for increased strain-induced splitting of valleys, we write the total electron mobility as

$$\hat{\mu}_n^{\text{tot}} = \sum_{i=1}^3 p^{(i)} \cdot \hat{\mu}_{n,\text{str}}^{(i)}. \quad (1)$$

Here the  $\hat{\mu}_{n,\text{str}}^{(i)}$  denotes the electron mobility tensors for strained Si for [100], [010], and [001] X-valleys corresponding to directions  $x$ ,  $y$ , and  $z$ , respectively. In (1) we model the mobility tensor as a product of a scalar mobility and the scaled inverse mass tensor.

$$\hat{\mu}_{n,\text{str}}^{(i)} = \mu \cdot \hat{m}_{(i)}^{-1}, \quad i = x, y, z \quad (2)$$

$$\hat{m}_x^{-1} = \begin{pmatrix} \frac{m_c}{m_l} & 0 & 0 \\ 0 & \frac{m_c}{m_t} & 0 \\ 0 & 0 & \frac{m_c}{m_t} \end{pmatrix} \quad (3)$$

$$\widehat{m}_y^{-1} = \begin{pmatrix} \frac{m_c}{m_t} & 0 & 0 \\ 0 & \frac{m_c}{m_l} & 0 \\ 0 & 0 & \frac{m_c}{m_t} \end{pmatrix} \quad (4)$$

$$\widehat{m}_z^{-1} = \begin{pmatrix} \frac{m_c}{m_t} & 0 & 0 \\ 0 & \frac{m_c}{m_t} & 0 \\ 0 & 0 & \frac{m_c}{m_l} \end{pmatrix} \quad (5)$$

The factor  $\mu$  includes the dependence on the energies  $\Delta E_C^{(i)}$  and the doping concentration  $N_I$  in the strained Si layer.

$$\mu(N_I, \Delta E_C^{(i)}) = \frac{q}{m_c \left( \frac{1}{\tau_{\text{equiv}}} + \frac{1}{\tau_{\text{neq}}(\Delta E_C^{(i)})} + \frac{1}{\tau_I(N_I)} \right)} \quad (6)$$

In (6)  $\tau_{\text{equiv}}$  denotes the momentum relaxation time due to acoustic intra-valley scattering and inter-valley scattering between equivalent valleys ( $g$ -type),  $\tau_{\text{neq}}(\Delta E_C^{(i)})$  for inter-valley scattering between non-equivalent valleys ( $f$ -type scattering), and  $\tau_I(N_I)$  for impurity scattering. The tensors in (2) are the inverse effective mass tensors with  $m_t$ ,  $m_l$  denoting the transversal and lateral masses for the ellipsoidal X-valleys in Si. The tensor is scaled to a dimensionless form by the conductivity mass,  $m_c$ .

$$m_c = \frac{3}{\frac{2}{m_t} + \frac{1}{m_l}} \quad (7)$$

To arrive at a formal description of the mobility components in strained Si, we modify the inter-valley scattering rate. The inter-valley scattering rate is a function of the strain-induced splitting of the valleys and can be expressed by a dimensionless factor  $h^{(i)}$ .

$$h^{(i)} = \frac{\tau_{\text{neq}}^0}{\tau_{\text{neq}}^{(i)}} = \frac{g(\Delta_{ij}^{\text{em}}) + g(\Delta_{il}^{\text{em}}) + e^{W_{\text{op}}} [g(\Delta_{ij}^{\text{ab}}) + g(\Delta_{il}^{\text{ab}})]}{2[g(-W_{\text{op}}) + \Gamma(\frac{3}{2})]} \quad (8)$$

$$\Delta_{ij}^{\text{em}} = \frac{\Delta E_C^{(j)} - \Delta E_C^{(i)}}{k_B T} - W_{\text{op}} \quad (9)$$

$$\Delta_{ij}^{\text{ab}} = \frac{\Delta E_C^{(j)} - \Delta E_C^{(i)}}{k_B T} + W_{\text{op}} \quad (10)$$

$$W_{\text{op}} = \frac{\hbar\omega_{\text{opt}}}{k_B T} \quad (11)$$

The function  $g$  is defined as

$$g(z) = \begin{cases} e^{-z} \cdot \Gamma(\frac{3}{2}) & \forall z > 0 \\ e^{-z} \cdot \Gamma(\frac{3}{2}, -z) & \forall z < 0 \end{cases} \quad (12)$$

Here  $\hbar\omega_{\text{opt}}$  denotes the phonon energy.  $\Gamma(\frac{3}{2}) = \frac{\sqrt{\pi}}{2}$  and  $\Gamma(\frac{3}{2}, -z)$  denotes the incomplete Gamma function. (8) describes the total inter-valley scattering rate for electrons to scatter from an initial valley  $i$  to final valleys  $j$  and  $l$ . Replacing the inter-valley term in (6) by (8), the electron mobility for the  $i^{\text{th}}$  valley in strained Si can be written as

$$\widehat{\mu}_{\text{n, str}}^{(i)}(N_I, y) = \mu^{\text{L}} \cdot \widehat{m}_{(i)}^{-1} \times \frac{\beta}{1 + (\beta - 1) \cdot h^{(i)}(y) + \beta \cdot \left( \frac{\mu^{\text{L}}}{\mu^{\text{LI}}} - 1 \right)} \quad (13)$$

where  $\widehat{m}_{(i)}^{-1}$  denotes the scaled effective mass tensor for the  $i^{\text{th}}$  valley in (2) and  $\beta = \frac{f \cdot m_t}{m_c}$ . The mobility enhancement factor  $f$  is defined as the ratio of the saturation electron mobility in strained Si to the unstrained mobility. The  $\mu^{\text{L}}$  and  $\mu^{\text{LI}}$  signify the lattice mobility and the lattice mobility including the effect of impurity scattering, respectively. Equation (13) is plugged into (1) to give the total mobility tensor for electrons in strained Si as a function of doping concentration  $N_I$  and strain. The tensor in (13) is given in the principle coordinate system and has a diagonal form.

#### IV. RESULTS AND DISCUSSION

In order to validate the model, Monte Carlo simulations were performed. The results obtained have been fit to experimental data which are available in the form of piezo-resistance coefficients. For low strain levels, the increase in the in-plane electron mobility is linear, characterized by the piezo resistance coefficients. Changing the shear deformation potential  $\Xi_u$  from 9.29eV [5] to 7.3eV gives good agreement for low strains.

Experimental and simulation results from other groups [6] [7] have indicated an approximate increase of 70% of the in-plane electron mobility in strained Si layers on SiGe [001] substrates, when compared to conventional Si. To achieve such values, it was required that the coupling constants of the  $g$ -type phonon be reduced by a factor of 1.2 and that for  $f$ -type phonons increased by a factor of 1.2, as compared to the original values proposed by Jacoboni [8]. The only parameter of the inter-valley scattering model (13) is the phonon energy. A value of  $\hbar\omega_{\text{opt}} = 60$  meV has been assumed. While the model based on piezo-resistance coefficients assumes a linear relationship between mobility

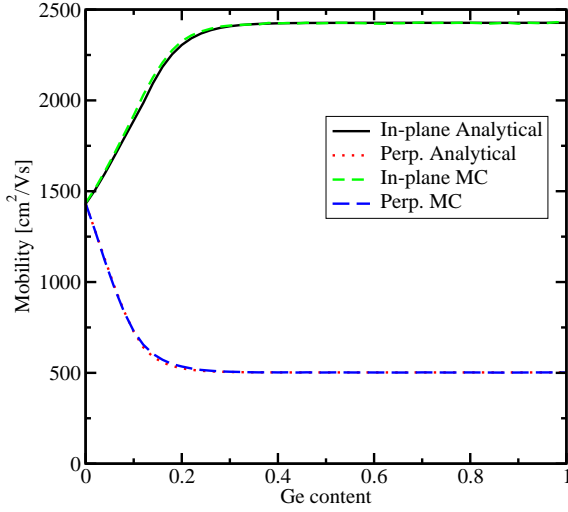


Fig. 2. In-plane and perpendicular electron mobilities in undoped strained Si versus the Ge content in SiGe [001] buffer layer .

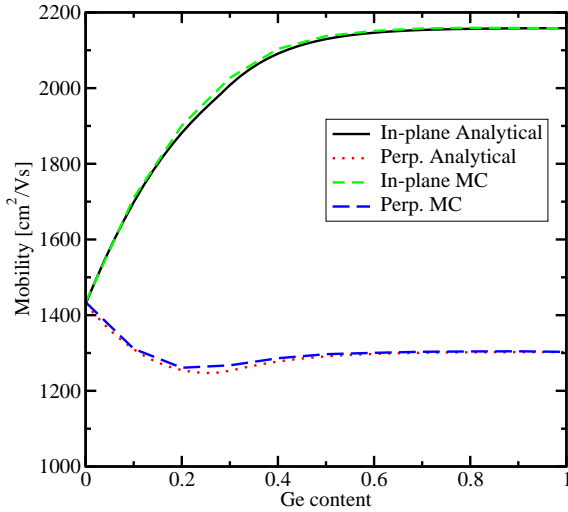


Fig. 3. In-plane and perpendicular electron mobilities in undoped strained Si versus the Ge content in SiGe [110] buffer layer .

enhancement and strain, for low strain levels, with the proposed model the mobility enhancement saturates at large strain values, as is observed experimentally.

The dependence of the electron mobility components on the orientation of the underlying SiGe layer is taken into account by performing a transformation of the strain tensor from the interface coordinate system to the principle coordinate system, using the transformation matrix as discussed in [9]. Fig. 2, Fig. 3 and Fig. 4 show the electron lattice mobility components for different strain levels obtained using (13) for substrate orientations [001], [110] and [123], respectively.

For substrate orientations [001], see Fig. 2, the two in-

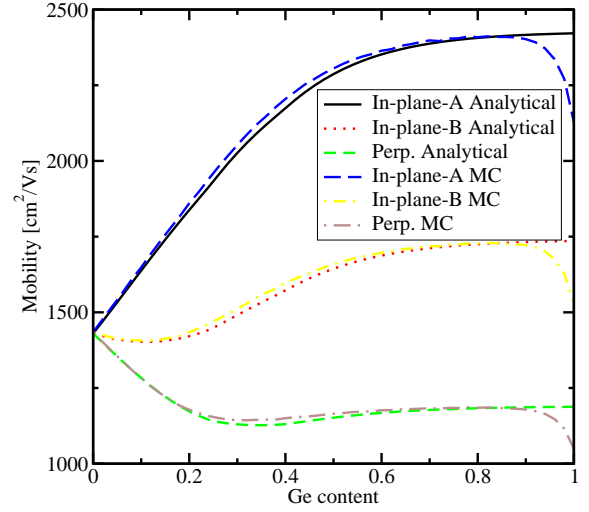


Fig. 4. In-plane and perpendicular electron mobilities in undoped strained Si versus the Ge content in SiGe [123] buffer layer .

plane components of electron mobility are equal. For [110] orientation, one of the in-plane components is equal to the perpendicular component, see Fig. 3. Three different components of the mobility can be clearly seen in Fig. 4 for the [123] orientation.

It is remarkable to see the excellent agreement between the MC simulation results and those obtained from our model for a large range of Ge content  $y$  in the SiGe layer. The deviation for very large strain levels (Ge content  $\geq 0.85$ ) is due to the fact that the proposed model does not consider the population of the L valleys for large Ge content.

The doping and material composition dependence of the in-plane and perpendicular electron mobilities in strained Si is calculated using (13) with the doping dependence of  $\mu^{LI}$  for electrons in Si given by [10]

$$\mu_{n,\min}^{LI} = \frac{\mu_n^L - \mu_{\min}^{\text{mid}}}{1 + \left(\frac{N_A}{C^{\text{mid}}}\right)^\eta} + \frac{\mu_{\min}^{\text{mid}} - \mu_{\min}^{\text{hi}}}{1 + \left(\frac{N_A}{C_{\min}^{\text{hi}}}\right)^\lambda} + \mu_{\min}^{\text{hi}} \quad (14)$$

where,  $\mu_n^L$  is the mobility for undoped material,  $\mu_{\min}^{\text{hi}}$  is the mobility at highest doping.  $\mu_{\min}^{\text{mid}}$ ,  $\mu_{\min}^{\text{hi}}$ ,  $C^{\text{mid}}$ ,  $C_{\min}^{\text{hi}}$ ,  $\eta$ , and  $\lambda$  are used as fitting parameters. The model parameters are summarized in Table 1.

Figure 5 and 6 show the doping dependence of the electron mobility components in strained Si layers for different Ge content in the underlying SiGe for [001] orientation of the substrate. The solid lines depict the results as obtained from our analytical model (13) while the symbols indicate the MC simulation results. As can be seen, with the increase in the doping concentration, the strain-

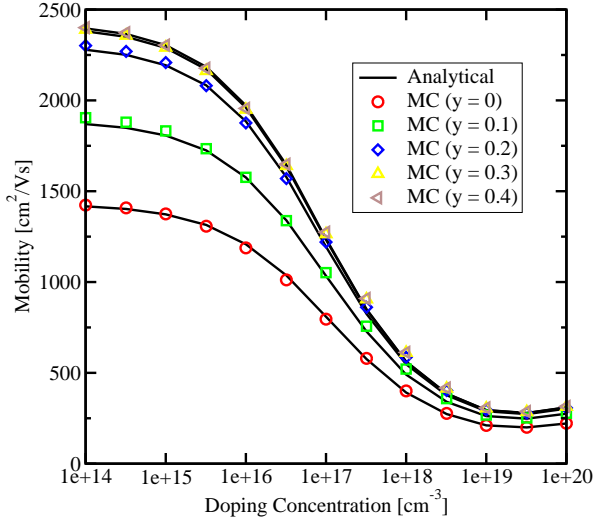


Fig. 5. Doping dependence of in-plane electron (minority) mobility in strained Si calculated using (13) for different Ge content in SiGe [001] substrate.

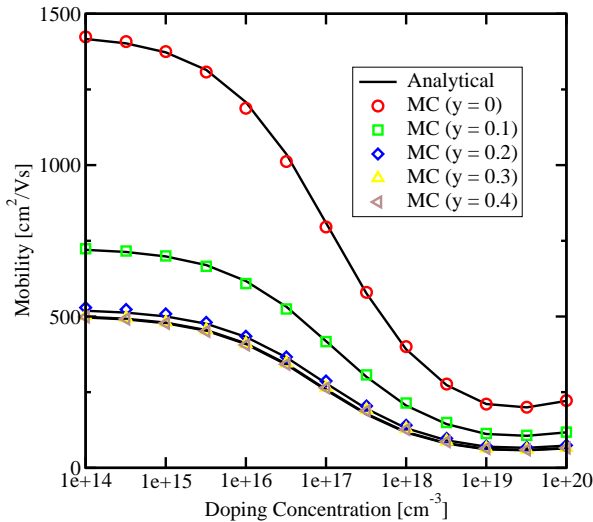


Fig. 6. Doping dependence of perpendicular electron (minority) mobility in strained Si calculated using (13) for different Ge content in SiGe [001] substrate.

induced enhancement of the electron mobility is gradually suppressed.

## V. CONCLUSION

An analytical model to describe the anisotropy of the electron mobility in strained Si has been developed. The model includes the effect of reduction of inter-valley scattering rate, through the equilibrium electron distribution and valley splitting. Results obtained from the model show excellent agreement with MC simulations for different SiGe substrate orientations and doping concentrations in the strained layer.

TABLE I  
PARAMETER VALUES FOR THE ELECTRON MOBILITY IN Si  
AT 300 K

Parameter	Si
$\mu_n^L$ [cm <sup>2</sup> /Vs]	1430
$\mu_{\min}^{\text{mid}}$ [cm <sup>2</sup> /Vs]	141
$\mu_{\min}^{\text{hi}}$ [cm <sup>2</sup> /Vs]	218
$\eta$	0.65
$\lambda$	2.0
$C_{\min}^{\text{mid}}$ [cm <sup>-3</sup> ]	1.12e17
$C_{\min}^{\text{hi}}$ [cm <sup>-3</sup> ]	4.35e19

## ACKNOWLEDGMENT

The authors would like to acknowledge the support from Semiconductor Research Corporation (SRC), project number 998.001 and Österreichische Forschungsgemeinschaft (ÖFG), Project MOEL-Plus 044.

## REFERENCES

- [1] L.-J. Huang, J. Chu, S. Goma, C.Emic, S. Koester, D. Canaperi, P. Mooney, S. Cordes, J. Speidell, R. Anderson, and H. Wong, "Carrier mobility enhancement in strained Si-on-Insulator fabricated by wafer bonding," in *VLSI Symp. Tech.Dig.*, 2001, pp. 57–58.
- [2] N. Sugii, D. Hisamoto, K. Washio, N. Yokoyama, and S. Kimura, "Enhanced performance of strained-Si MOSFETs on CMP SiGe virtual substrate," in *IEDM Tech.Dig.*, 2001, pp. 737–740.
- [3] S. Ito *et al.*, "Mechanical stress effect of etch-stop nitride and its impact on deep submicron transistor design," in *IEDM Tech.Dig.*, 2000, pp. 247–251.
- [4] A. Shimizu *et al.*, "Local mechanical-stress control (lmc) : A new technique for cmos performance enhancement," in *IEDM Tech.Dig.*, 2001, pp. 433–437.
- [5] M. Rieger and P. Vogl, "Electronic-band parameters in strained Si<sub>1-x</sub>Ge<sub>x</sub> alloys on Si<sub>1-y</sub>Ge<sub>y</sub> substrates," *Phys.Rev.B*, vol. 48, no. 19, pp. 14 276–14 287, 1993.
- [6] Z.-Y. Cheng *et al.*, "Electron mobility enhancement in strained-Si n-MOSFETs fabricated on SiGe-on-Insulator(SGOI) substrates," *IEEE Electron Device Lett.*, vol. 22, no. 7, pp. 321–323, 2001.
- [7] S. Takagi, J. Hoyt, J. Welser, and J. Gibbons, "Comparative study of phonon-limited mobility of two-dimensional electrons in strained and unstrained Si metal-oxide-semiconductor field-effect transistors," *J.Appl.Phys.*, vol. 80, no. 3, pp. 1567–77, 1996.
- [8] C. Jacoboni and L. Reggiani, "The Monte Carlo method for the solution of charge transport in semiconductors with applications to covalent materials," *Review of Modern Physics*, vol. 55, pp. 645–705, 1983.
- [9] S. Smirnov and H. Kosina, "Monte Carlo modeling of the electron mobility in strained Si<sub>1-x</sub>Ge<sub>x</sub> layers on arbitrarily oriented Si<sub>1-y</sub>Ge<sub>y</sub> substrates," *Solid State Electronics*, vol. 48, no. 1-4, pp. 1325–1335, 2004.
- [10] V. Palankovski and R. Quay, *Analysis and Simulation of Heterostructure Devices*. Wien, New York: Springer, 2004.